Chain stretching effect on the morphology and kinetics of microphase separation of diblock copolymer under simple shear flow

ARTICLE *in* THE JOURNAL OF CHEMICAL PHYSICS · AUGUST 2001

Impact Factor: 2.95 · DOI: 10.1063/1.1384420

2 AUTHORS, INCLUDING:

Kaifu Luo
University of Science and Technology of China
44 PUBLICATIONS **1,163** CITATIONS

Chain stretching effect on the morphology and kinetics of microphase separation of diblock copolymer under simple shear flow

Kaifu Luo
Department of Macromolecular Science, The Key Laboratory of Molecular Engineering of Polymers, SMEC, Fudan University, Shanghai 200433, China

Yuliang Yang[a)]
Department of Macromolecular Science, The Key Laboratory of Molecular Engineering of Polymers, SMEC and Department of Physics, Fudan University, Shanghai 200433, China

(Received 11 January 2001; accepted 16 May 2001)

By incorporating the information of chain conformation into the free-energy calculation, the chain stretching effect on the morphology and kinetics of microphase separation of symmetric diblock copolymers under simple shear flow is investigated based on the time-dependent Ginzburg–Landau model. We first showed that the order–disorder transition (ODT) temperature increases with $\tau_1\dot{\gamma}$, where τ_1 is the Rouse terminal relaxation time and $\dot{\gamma}$ is the shear rate. The simulation results show that τ_1 and $\dot{\gamma}$ play the central role in the morphology of microphase separated diblock copolymers. It is found that, for the case without chain stretching effect ($\tau_1\dot{\gamma}=0$), perpendicular (with the lamella normal perpendicular to the flow direction and the velocity gradient direction) and parallel (with the lamella normal parallel to the velocity gradient direction) alignments are obtained for shallow and deep quenches, respectively. However, when the chain stretching effect is strong, i.e., high $\tau_1\dot{\gamma}$, the undulated lamella transverse alignment (with the lamella normal parallel to the flow direction) can be observed. The processes of morphology forming and the lamella undulation are discussed based on the anisotropic growth of the correlation lengths. © *2001 American Institute of Physics.* [DOI: 10.1063/1.1384420]

I. INTRODUCTION

Research on complex fluids, such as polymers, emulsions, and colloidal suspensions, is now one of the most active fields in condensed-matter physics.[1,2] The pattern formation dynamics of order–disorder transitions (ODT) of block copolymers has been an important example. The simplest block polymer is diblock polymer, which is formed by connecting two sequences of A and B monomers. Diblock copolymer melts have received much attention over the past years due in large part to their ability to self-assemble into a variety of ordered microstructures.[1,2]

The ODT of diblock copolymers was first theoretically studied by Leibler in the mean-field (MF) frame,[3] and later by Fredrickson and Helfand[4] and Ohta and Kawasaki.[5,6] Contrary to current theories, Bates *et al.*[7] have found that the Gaussian-to-stretched coil transition occurs well below the ODT. Later, they introduce a dimensionless distance D of separation between A and B blocks, and formulate a block copolymer theory that accounts for chain stretching on the basis of Leibler's random phase approximation (RPA) theory.[8]

Current interest has turned toward understanding flow-induced alignment microstructures. As to symmetrical diblock copolymer, by varying the shearing conditions and the temperature, the ''parallel alignment,'' i.e., lamellar normal is parallel to the velocity gradient direction,[9,10] ''perpendicular alignment'' and ''transverse alignment'' in which the lamellar normals are parallel to the vortex direction,[11,12] and to the velocity direction,[13] respectively, have been observed. In spite of these considerable experimental advances, the mechanism for flow-induced lamella alignment has not been well understood. The primary theory of ODT under simple shear flow was developed in the past decade. Fredrickson[14] first studied the scattering function of a diblock copolymer in the presence of a steady homogeneous flow field with a simplified stochastic model which can be derived from the models employed by Onuki and Kawasaki.[15] Fredrickson found that simple shear can suppress concentration fluctuations in disordered block copolymer and render the fluctuation spectrum highly anisotropic. Subsequently, several papers[16–18] were published on the issue of the rheological properties of homogeneous diblock copolymer melts affected by the shear-induced suppression of fluctuations. By applying a self-consistent Hartree approximation to the nonequilibrated system, Cates and Milner[19] studied the role of shear in the isotropic–lamella transition and first formulated the concept that the attenuation of the fluctuation field induced by shear drives the system towards the mean-field limit and eventually the disordered copolymer melts become less stable, which results in an apparent increase of the ODT temperature. Later, Fredrickson[20] modified the theory of Cates and Milner to incorporate different viscosity of the pure block components, and restored some neglected couplings between the mean composition pattern and composition fluctuation about the mean. Many qualitative features of experimental observations were reproduced. In particular, perpendicular lamellae were predicted to be stable at ODT under strong

a)Author to whom correspondence should be addressed. Electronic mail: ylyang@srcap.stc.sh.cn

shear condition, while lowering the temperature induced a transition to parallel lamellae. Huang and Muthukumar[21] solved numerically the self-consistent equation for composition fluctuation in diblock and triblock copolymer systems under a steady simple shear flow, and calculated the induced ODT and OOT (order–order transition) due to the attenuation of the fluctuation field caused by the external hydrodynamic field. Their results are not only in good agreement with the previous theories and the experimental data, but also resolve the earlier controversy arising from the discrepancy between them.

However, all the theoretical studies mentioned above are not applicable to the case of high shear rate, because the chain coil will be stretched and oriented along the shear flow direction, especially for chains with long terminal relaxation times, under high shear rate. It is not difficult to understand that the deformation of chain conformation will affect the microphase separation dynamics and the morphologies. But, to our knowledge, nobody has incorporated the chain conformation effect on the morphology evolution and kinetics of diblock copolymers under shear flow.

For polymer blends, however, several approaches[22–24] have been proposed to explain the flow effect by modifying the mean-field- or Flory–Huggins free energy to include elastic energy of deformation produced by the flow. But, these approaches are largely phenomenological in the sense that they don't directly relate the stored elastic energy to the chain conformation statistics. To overcome this disadvantage, Bhttacharjee *et al.*[25] have introduced conformation statistics to study the phase separation of polymer solutions in the elongational flow. Pistoor and Binder[26] derived the free-energy functional of binary polymer mixtures under simple shear flow, including the stored entropic elastic energy originated from chain stretching. Based on this free-energy functional, Qiu and Yang[27,28] have demonstrated both experimentally and theoretically that the chain stretching due to the flow field will alter the dynamics, morphology, and rheological properties for a phase separating polymer blends. The results show that,[28] for higher value of Rouse terminal relaxation times, the domain burst due to the surface tension is suppressed and the domains are highly elongated and form the string-like patterns observed experimentally under strong shear. Following the theoretical and experimental results mentioned above, it is obvious that the chain stretching effect will also play important roles on the ODT, dynamics, morphology, and related rheological properties of diblock copolymers.

The time-dependent Ginzburg–Landau (TDGL) model is frequently used to numerically simulate the kinetics and morphology of diblock copolymer systems. Unfortunately, in most simulations based on TDGL model it is assumed that the characteristic time scales of external flow and the phase separation are substantially longer than the terminal relaxation time of the chain. However, this assumption fails when the flow rate is higher or comparable to the inverse of the chain terminal relaxation time. In this case, the detailed information of chain conformation under macroscopic flow should be included. The main objective of the present study is to investigate the effect of chain stretching on the ODT, kinetics, morphologies, and corresponding rheological properties of diblock copolymers under simple shear flow.

The following treatment is based on the assumptions that the polymer chains are not too long, so that the simple Rouse model[29] is sufficient to describe the dynamics of polymers in the melt,[26] and the mobility coefficients of two blocks are the same. In the next section, the free-energy functional for the diblock copolymer under simple shear flow, in which the conformation of a Rouse coil under shear flow is included, is derived. The derived free-energy functional will be incorporated into the TDGL equation in $\mathbf{q}$ space to solve the order parameter field in $\mathbf{q}$ space, $\psi(\mathbf{q},t)$. The morphological evolution of the system, $\psi(\mathbf{r},t)$, is obtained by inverse Fourier transformation of $\psi(\mathbf{q},t)$.

II. THEORY

A. Deformation of diblock copolymer coil under shear flow and its effect on ODT

Assume that the block copolymer chain has $N=N_A+N_B$ Gaussian statistical segments, where $N_A \gg 1$ and $N_B \gg 1$ denote the number of monomers of type A and B, respectively. The composition of the chain is defined as $f=N_A/N$. For simplicity, for both blocks, the same Kuhn length, i.e., $\sigma_A=\sigma_B=\sigma$, is assumed. Following Leibler theory,[3] in the limit of zero compressibility the free-energy functional can be written as

$$
\begin{aligned}
F[\psi(\mathbf{q})] = & \frac{1}{2}\int d\mathbf{q}\,\Gamma_2(\mathbf{q},-\mathbf{q})\psi(\mathbf{q})\psi(-\mathbf{q}) + \frac{1}{3!}\int d\mathbf{q}_1 \\
& \times \int d\mathbf{q}_2\,\Gamma_3(\mathbf{q}_1,\mathbf{q}_2,-\mathbf{q}_1-\mathbf{q}_2)\psi(\mathbf{q}_1)\psi(\mathbf{q}_2) \\
& \times \psi(-\mathbf{q}_1-\mathbf{q}_2) + \frac{1}{4!}\int d\mathbf{q}_1 \int d\mathbf{q}_2 \int d\mathbf{q}_3 \\
& \times \Gamma_4(\mathbf{q}_1,\mathbf{q}_2,\mathbf{q}_3,-\mathbf{q}_1-\mathbf{q}_2,-\mathbf{q}_3)\psi(\mathbf{q}_1)\psi(\mathbf{q}_2) \\
& \times \psi(\mathbf{q}_3)\psi(-\mathbf{q}_1-\mathbf{q}_2-\mathbf{q}_3) + \cdots, \qquad (1)
\end{aligned}
$$

where $\psi(\mathbf{q})$ is the Fourier transform of the order parameter $\psi(\mathbf{r})=\rho_A(\mathbf{r})/\rho - f$ with $\rho_A(\mathbf{r})$ the local density of A segments at point $\mathbf{r}$ and ρ the overall average segment's density. For the symmetric diblock copolymer under the random phase approximation (RPA), it is obtained that $\Gamma_2(\mathbf{q},-\mathbf{q})=S^{-1}(\mathbf{q})$, and $\Gamma_3(\mathbf{q}_1,\mathbf{q}_2,-\mathbf{q}_1-\mathbf{q}_2)=0$. However, $\Gamma_4(\mathbf{q}_1,\mathbf{q}_2,\mathbf{q}_3,-\mathbf{q}_1-\mathbf{q}_2-\mathbf{q}_3)$ is very complex, and it is assumed to be a constant in the following discussion. Following Leibler, the RPA scattering function $S(\mathbf{q})$ for the diblock polymer can be written as[3]

$$
S^{-1}(\mathbf{q}) = \frac{T(\mathbf{q})}{W(\mathbf{q})} - 2\chi, \qquad (2)
$$

where χ is the Flory–Huggins parameter used to describe the effect of enthalpy of nonbonded interactions; $W(q)$ and $T(q)$ can be further expressed by partial structure factors, i.e.,

$$
W(\mathbf{q}) = S_{AA}(\mathbf{q})S_{BB}(\mathbf{q}) - S_{AB}^2(\mathbf{q}), \qquad (3)
$$

$$T(\mathbf{q}) = S_{AA}(\mathbf{q}) + S_{BB}(\mathbf{q}) + 2S_{AB}(\mathbf{q}). \tag{4}$$

Therefore, in order to obtain the free-energy functional in the presence of shear flow, the key step is to derive these partial structure factors with the chain stretching effect.

For simplicity, the conventional Rouse model is used.[30,31] We must note that the Rouse model can be readily applied to the dynamics of polymer melts when the molecular weight is lower than the critical molecular weight for the occurrence of entanglement.

First, we consider a Rouse chain consisting of N beads with coefficient ζ connected by Hookean springs with spring constant k. It is well known that $k = 3k_BT/\sigma^2$, where σ is the Kuhn length of the chain, and k_BT is the Boltzmann constant times the absolute temperature. Then, the distribution function Ψ, describing the configuration of the coil, is conveniently expressed in normal coordinates $\mathbf{Q}_p[\mathbf{Q}_p \equiv (\mathbf{X}'_p, \mathbf{Y}'_p, \mathbf{Z}'_p)]$ $(p = 1,...,N-1)$ and satisfies the Smoluchowski equation[32]

$$\frac{\partial \Psi}{\partial t} = \sum_p \frac{1}{\zeta_p} \frac{\partial}{\partial \mathbf{Q}_p} \cdot \left(k_BT \frac{\partial}{\partial \mathbf{Q}_p} \Psi + k_p \mathbf{Q}_p \Psi \right) - \sum_p \frac{\partial}{\partial \mathbf{Q}_p} (\aleph \cdot \mathbf{Q}_p) \Psi, \tag{5}$$

where

$$\zeta_0 = N\zeta, \quad \zeta_p = 2N\zeta \quad (p = 1,2,...,N-1), \tag{6}$$

$$k_p = 2\pi^2 k p^2/N = \frac{6\pi^2 k_B T}{N\sigma^2} p^2 \quad (p = 0,1,2,...,N-1). \tag{7}$$

The matrix $\aleph$ in Eq. (5) represents the flow $\mathbf{v} = \aleph \cdot \mathbf{r}$, which, for the case of simple shear flow, yields

$$\aleph = \begin{pmatrix} 0 & \dot{\gamma} & 0 \\ 0 & 0 & 0 \\ 0 & 0 & 0 \end{pmatrix}, \tag{8}$$

where $\dot{\gamma}$ is the shear rate. The Smoluchowski equation for the probability distribution function of a single molecule has an analytical nonequilibrium steady solution[33]

$$\Psi \propto \exp\left[-\sum_p \frac{k_p}{2k_BT} \frac{\{\mathbf{X}'^2_p - 2\tau_p \dot{\gamma} \mathbf{X}'_p \mathbf{Y}'_p + (1 + 2\tau_p^2 \dot{\gamma}^2) \mathbf{Y}'^2_p + (1 + \tau_p^2 \dot{\gamma}^2) \mathbf{Z}'^2_p\}}{1 + \tau_p^2 \dot{\gamma}^2} \right], \tag{9}$$

where τ_p denotes the relaxation times

$$\tau_p^{-1} = \frac{24 k_BT}{\zeta \sigma^2} \sin^2 \frac{p\pi}{2N} \approx \tau_1 / p^2, \tag{10}$$

with τ_1 being the longest Rouse internal mode relaxation time. By introducing the following new coordinates:

$$\mathbf{X}_p = \frac{(\mathbf{X}'_p - \tau_p \dot{\gamma} \mathbf{Y}'_p)}{\sqrt{1 + \tau_p^2 \dot{\gamma}^2}}, \quad \mathbf{Y}_p = \mathbf{Y}'_p, \quad \mathbf{Z}_p = \mathbf{Z}'_p. \tag{11}$$

The distribution function Ψ becomes

$$\Psi \propto \exp\left[-\sum_p \frac{k_p}{2k_BT} (\mathbf{X}_p^2 + \mathbf{Y}_p^2 + \mathbf{Z}_p^2) \right]. \tag{12}$$

Now, according to the above distribution function Ψ of the Rouse chain under simple shear flow, we can take into account the diblock copolymer chain. We assume that the friction coefficients for both blocks are almost the same, i.e., $\zeta_A \approx \zeta_B \approx \zeta$. This assumption substantially simplifies the following derivation. For a diblock copolymer, partial structure factors are written as

$$S_{AA}(\mathbf{q}) = \frac{1}{N} \sum_{n=1}^{fN} \sum_{m=1}^{fN} \langle \exp[i\mathbf{q} \cdot \mathbf{r}_{mn}] \rangle = \frac{1}{N} \sum_{n=1}^{fN} \sum_{m=1}^{fN} \exp[-g(m,n,\mathbf{q},\dot{\gamma})], \tag{13}$$

$$S_{BB}(\mathbf{q}) = \frac{1}{N} \sum_{n=fN+1}^{N} \sum_{m=fN+1}^{N} \langle \exp[i\mathbf{q} \cdot \mathbf{r}_{mn}] \rangle = \frac{1}{N} \sum_{n=fN+1}^{N} \sum_{m=fN+1}^{N} \exp[-g(m,n,\mathbf{q},\dot{\gamma})], \tag{14}$$

$$S_{AB}(\mathbf{q}) = \frac{1}{N} \sum_{n=1}^{fN} \sum_{m=fN+1}^{N} \langle \exp[i\mathbf{q} \cdot \mathbf{r}_{mn}] \rangle = \frac{1}{N} \sum_{n=1}^{fN} \sum_{m=fN+1}^{N} \exp[-g(m,n,\mathbf{q},\dot{\gamma})], \tag{15}$$

where

$$\mathbf{r}_{mn} = 2 \sum_{p=1}^{\infty} \mathbf{Q}_p \left[\cos\left(\frac{p\pi n}{N} \right) - \cos\left(\frac{p\pi m}{N} \right) \right], \tag{16}$$

and

$$g(m,n,\mathbf{q},\dot{\gamma}) = \frac{N\sigma^2}{3\pi^2}\sum_{p=1}^{N-1}\frac{1}{p^2}\left[\cos\left(\frac{p\pi n}{N}\right)-\cos\left(\frac{p\pi m}{N}\right)\right]^2 \times(2\tau_p^2\dot{\gamma}^2q_x^2+2\tau_p\dot{\gamma}q_xq_y+q^2) \approx \frac{N\sigma^2}{3\pi^2}\sum_{p=1}^{N-1}\frac{1}{p^2}\left[\cos\left(\frac{p\pi n}{N}\right)-\cos\left(\frac{p\pi m}{N}\right)\right]^2 \times(2\tau_1^2\dot{\gamma}^2q_x^2/p^4+2\tau_1\dot{\gamma}q_xq_y/p^2+q^2). \tag{17}$$

It is clear that $g(m,n,\mathbf{q},\dot{\gamma})$ is anisotropic and its anisotropy is measured by the value of $\tau_1\dot{\gamma}$. However, $g(m,n,\mathbf{q},\dot{\gamma})$ is isotropic when $q_x=0$, and thus $S(\mathbf{q})$ is isotropic in the scattering plane (q_y,q_z) even in the presence of shear flow.

It is known that, in the regime of $qR_G\ll 1$, where R_G is the Gaussian radius of gyration of the whole chain, the function of $\exp[-g(m,n,\mathbf{q},\dot{\gamma})]$ can be expanded in terms of $q_i(i=x,y,z)$. By using this expansion, Pistoor and Binder[26] derived expressions for the chain deformation under the simple shear flow and its effect on the collective scattering functions for polymer blends. However, for the microphase separation in diblock copolymers, the maximum of $S(\mathbf{q})$ is approximately located at $qR_G\sim 4.0$ or larger for all compositions,[3] thus, the condition of $qR_G\ll 1$ can never be satisfied. Thus, for obtaining all the partial structure factors, the numerical computation is necessary.

We should mention that it is a formidable task to investigate the chain stretching effect on the ODT temperature by numerically searching the global minimum of $(T(\mathbf{q})/W(\mathbf{q}))$ and calculating the value of a parameter Δ for various $\tau_1\dot{\gamma}$ values, where Δ is the temperature-like parameter defined as $\min(T(\mathbf{q})/W(\mathbf{q}))_0-\min(T(\mathbf{q})/W(\mathbf{q}))_{\tau_1\dot{\gamma}}$. Here, the term $\min(T(\mathbf{q})/W(\mathbf{q}))_0=10.495$ corresponds to situation for $\tau_1\dot{\gamma}=0$. The numerical results reveal, in the (q_x,q_y) plane, two minimum values of $(T(\mathbf{q})/W(\mathbf{q}))_{\tau_1\dot{\gamma}}$ located in the first and third quadrants with the reflection symmetry. The symmetry axis tilts away from the q_x axis with angle of $-\theta$. In the limit of $\tau_1\dot{\gamma}\gg 1$, θ tends to be zero. In the (q_x,q_z) plane, two minimum values are located at $(\pm q_x,0)$. However, in the plane of (q_y,q_z), the coordinates of the minimum value consists of a circle due to the isotropy of $S(\mathbf{q})$ when $q_x=0$. The numerical results for the global minimum values are shown in Fig. 1. It is seen from Fig. 1 that Δ increases with $\tau_1\dot{\gamma}$, which indicates that with the increase of $\tau_1\dot{\gamma}$, the ODT temperature increases. More quantitatively, Fig. 1 shows that $\Delta\sim(\tau_1\dot{\gamma})^{1.0}$ when $\tau_1\dot{\gamma}\ll 1.0$ and it levels off when $\tau_1\dot{\gamma}\gg 1.0$.

We must point out that the Rouse model can be used assuming sufficiently low molecular weight diblock copolymer, and the mean-field theory is accurate at high molecular weights. So, our free-energy calculation is most appropriate at intermediate segregation just below the entanglement molecular weight.

B. Order parameter fluctuations in the presence of steady flow

In the presence of shear flow, the kinetic equation of the order parameter fluctuation for a diblock copolymer is written as

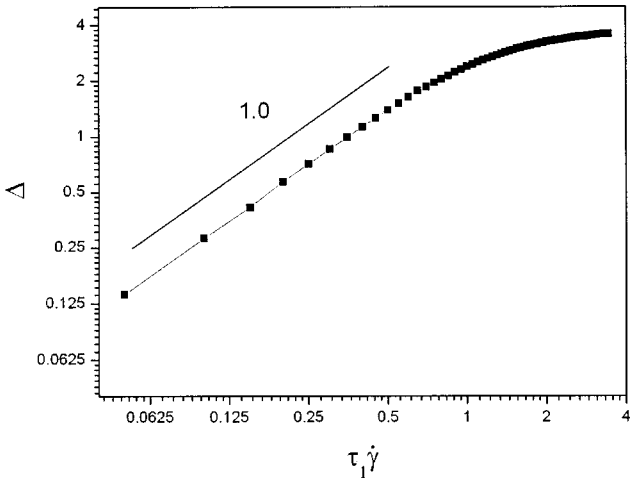

FIG. 1. Double logarithmic plot of the Δ vs $\tau_1\dot{\gamma}$.

$$\frac{\partial\psi(\mathbf{q})}{\partial t}-\dot{\gamma}q_x\frac{\partial\psi(\mathbf{q})}{\partial q_y}=-M(\mathbf{q})q^2\frac{\delta F[\psi(\mathbf{q})]}{\delta\psi(\mathbf{q})}+\eta(\mathbf{q},t), \tag{18}$$

where the stochastic force $\eta(\mathbf{q},t)$ is related to Onsager coefficient $M(\mathbf{q})$ via a fluctuation-dissipation theorem

$$\langle\eta(\mathbf{q},t)\,\eta(-\mathbf{q},t')\rangle=2M(\mathbf{q})q^2\delta(t-t'). \tag{19}$$

For simplicity, we neglect the $\mathbf{q}$ dependence of M, i.e., M is assumed to be a constant. Here, we should mention that Eq. (18) can only be used to describe dynamics of the order parameter on time scales longer than Rouse terminal relaxation time.

III. SIMULATION ALGORITHM

In order to investigate the morphological evolution of microphase separation, Eq. (18) is adopted. For the ease of simulation we neglect the noise term, which is only important at very early stage of microphase separation; Eq. (18) is then simplified to

$$\frac{\partial\psi(\mathbf{q})}{\partial t}-\dot{\gamma}q_x\frac{\partial\psi(\mathbf{q})}{\partial q_y} =-Mq^2\left(\frac{T(\mathbf{q})}{W(\mathbf{q})}\psi(\mathbf{q})+(a\psi(\mathbf{r})+b\psi^3(\mathbf{r}))_q\right), \tag{20}$$

where $(a\psi+b\psi^3)_q$ represents the Fourier transform of the bulk driving force term $a\psi+b\psi^3$. In the following simulation, we set $M=1.0$. To solve Eq. (20), the semi-implicit Fourier spectral method is used.[34,35] If we write $a\psi+b\psi^3$ as $f(\psi(\mathbf{r}))$, the explicit Euler Fourier spectral algorithm is written as

$$\psi^{n+1}(\mathbf{q},t)=\psi^n(\mathbf{q},t)-\Delta tq^2\{f(\psi(\mathbf{r}))\}_q^n -\Delta tq^2\left(\frac{T(\mathbf{q})}{W(\mathbf{q})}\right)\psi^n(\mathbf{q},t) +\frac{\Delta t}{2\Delta q_y}\dot{\gamma}q_x[\psi^n(q_x,q_y+\Delta q_y,q_z,t) -\psi^n(q_x,q_y-\Delta q_y,q_z,t)]. \tag{21}$$

The accuracy in time can be improved by using a higher-order semi-implicit Fourier spectral scheme. For instance, when a second-order backward difference (BDF) for $[\partial\psi(\mathbf{q},t)]/\partial t$ and a second-order Adams–Bashforth (AB) for the explicit treatment of a nonlinear term were applied to Eq. (20), the following second-order BDF/AB scheme is written as[34,35]

$$\left(3+2\Delta t q^2\left(\frac{T(\mathbf{q})}{W(\mathbf{q})}\right)\right)\psi^{n+1}(\mathbf{q},t)$$
$$=4\psi^n(\mathbf{q},t)-\psi^{n-1}(\mathbf{q},t)-2\Delta t q^2[2\{f(\psi(\mathbf{r}))\}_q^n$$
$$-\{f(\psi(\mathbf{r}))\}_q^{n-1}]+\frac{\Delta t}{\Delta q_y}\dot{\gamma}q_x[2(\psi^n(q_x,q_y+\Delta q_y,q_z,t)$$
$$-\psi^n(q_x,q_y-\Delta q_y,q_z,t))(\psi^{n-1}(q_x,q_y+\Delta q_y,q_z,t)$$
$$-\psi^{n-1}(q_x,q_y-\Delta q_y,q_z,t))]. \quad (22)$$

In our simulation, the system is confined in a $64\times64\times64$ cubic lattice, and we set $\Delta q_y=2\pi/64$, $q_\alpha=(2\pi/64)(i-33)$, $(\alpha=x,y,z,\ i=1,2,...,64)$. The system was initially prepared in a homogeneous state by assigning a random number to each lattice site. We may use Eq. (21) to compute $\psi^1(\mathbf{q},t)$, and hence $\{f(\psi(\mathbf{r}))\}_q^1$, which are needed to start the iteration in Eq. (22). In our simulation, the parameters are fixed as $f=0.5$, $N=100$, $\sigma^2=1.5$, and $\Delta t=0.5$. The parameter b is defined as $b=(1-a)/3$, with $a=2\chi$ in our case. An average was performed over four independent simulation runs with a different set of random numbers for each initial state. The temporal evolution of morphological pattern $\psi(\mathbf{r},t)$ shown in Figs. 2, 3, and 5 were obtained by inverse Fourier transform of $\psi(\mathbf{q},t)$.

The correlation lengths at time t in different directions, $R(x,t)$, $R(y,t)$, and $R(z,t)$, are calculated by[36,37]

$$R(\alpha,t)=\left[\frac{\int d\mathbf{q}\, q_\alpha^2 S(\mathbf{q},t)}{\int d\mathbf{q}\, S(\mathbf{q},t)}\right]^{-1/2}, \qquad \alpha=x,y,z, \quad (23)$$

where $S(\mathbf{q},t)=\langle\psi(\mathbf{q},t)\psi(-\mathbf{q},t)\rangle$ is the structure factor at the evolution time t.

IV. RESULTS AND DISCUSSIONS

A. The temporal evolution of morphological patterns

The microphase separation for the case of shallow quench ($\chi N=12.0$) and shear rate $\dot{\gamma}=0.001\ \mathrm{s}^{-1}$ is shown in Fig. 2. Figure 2(a), shows the morphological evolution for the case of $\tau_1\dot{\gamma}=0$ in which the chain terminal relaxation time $\tau_1=0$ and corresponds to the case of no chain stretching effect. It can be seen from Fig. 2(a) that the orientation of the lamellar normal is perpendicular to the flow axis (x) and parallel to the vorticity axis (z) when the shear strain $\gamma=\dot{\gamma}t\sim10.0$. This kind of lamellar alignment is called ''perpendicular alignment'' in the literature.[11–13,38,39] We must point out that, when $\tau_1\dot{\gamma}<0.1$, the coil is only slightly deformed, i.e., the chain is not stretched,[26] and thus the morphologies are very similar to the case of $\tau_1\dot{\gamma}=0$. However, when $\tau_1\dot{\gamma}>0.1$ (for example, $\tau_1\dot{\gamma}=0.75$) and $\dot{\gamma}=0.001\ \mathrm{s}^{-1}$, the chain coil deformation is substantial and its effect on the morphology of microphase separation of diblock copolymers is clearly seen from Figs. 2(b) and 2(c). It can be seen that, when the shear rate is high enough or the chain terminal relaxation time is long enough, the chain coil will be elongated along the flow direction. Therefore, the thermodynamic potential drives the system to form lamellar morphology and the flow field stretches the chain coil along the flow direction (x direction). These two effects result in the normal of the phase separated lamellar structure orienting along the flow direction, Figs. 2(b) and 2(c). This type of lamellar orientation is called ''transverse alignment'' in the literature.[13] An interesting phenomenon during the formation of transverse alignment is that the lamellae in the $x-y$ plane undulate. It implies that the transverse alignment is not stable due to the floating of the stretched diblock copolymer chains along the direction of steady shear flow. The detailed undulation process will be discussed in the next subsection. However, one can conjecture that this transverse lamella alignment can be stabilized under large amplitude oscillatory shear flow with zero net shear strain. In fact, Zhang and Wiesner[13] have observed this transverse alignment state, and the authors suggest that the chain stretching due to the topological constraints is responsible for this new type of alignment. We think that their experimental finding agrees with our simulation result.

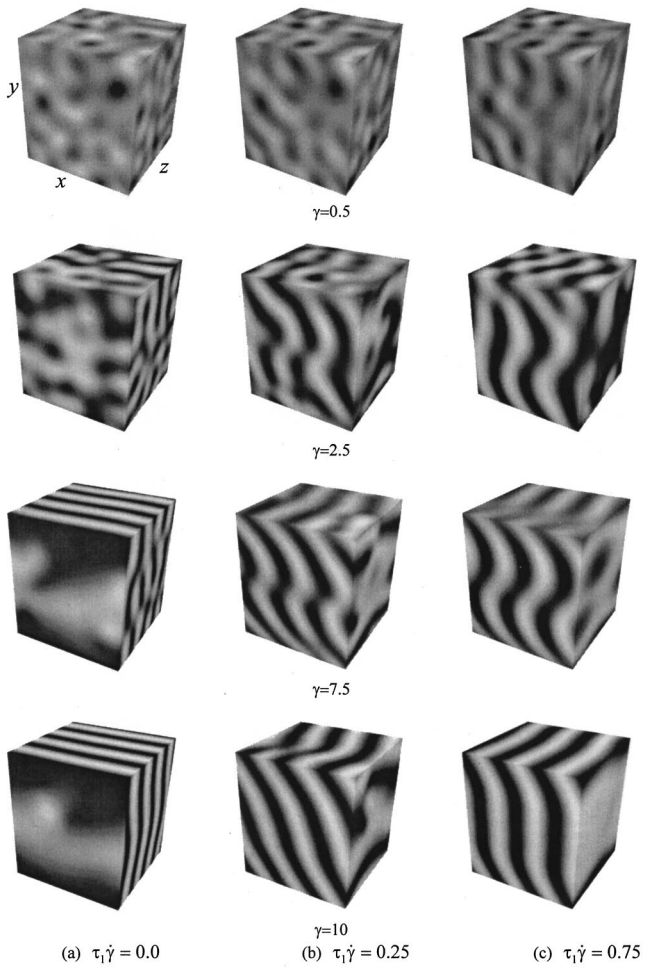

FIG. 2. The simulated morphological evolution of the symmetric diblock copolymer with quench depth $\chi N=12.0$ and shear rate $\dot{\gamma}=0.001\ \mathrm{s}^{-1}$ for different $\tau_1\dot{\gamma}$.

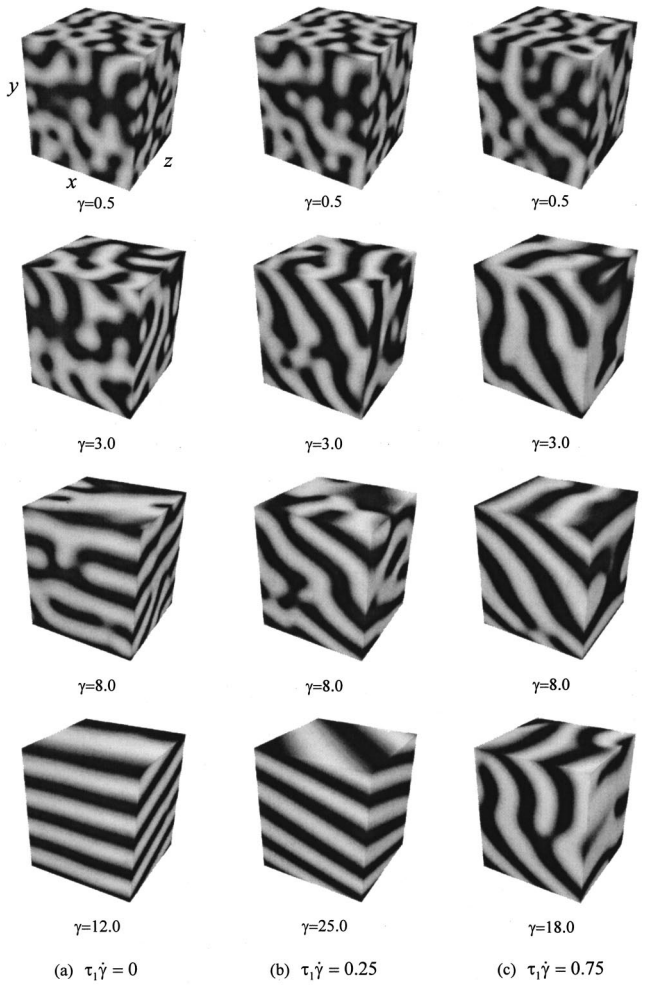

FIG. 3. The simulated morphological evolution of the symmetric diblock copolymer with quench depth $\chi N=20.0$ and shear rate $\dot{\gamma}=0.001\,\mathrm{s}^{-1}$ for different $\tau_1\dot{\gamma}$.

Now, we turn to discuss the case of deep quench. We set $\chi N=20.0$, and the shear rate $\dot{\gamma}=0.001\,\mathrm{s}^{-1}$. When the chain stretching effect is absent, i.e., $\tau_1\dot{\gamma}=0$, in contrast to the perpendicular alignment observed for shallow quench shown in Fig. 2(a), the parallel alignment is observed, Fig. 3(a). Our simulation results for the case without chain stretching effect are also consistent with Fredrickson's prediction[20] that the perpendicular lamellae are stable at high shear stress and for temperatures just below ODT, while parallel lamellae are favored under conditions of weak shear stress or low temperatures. It is known from both experiment and theoretical simulation that the sharp interface formed in deep quench will prefer the occurrence of parallel alignment.[13,38,39] However, when the chain terminal relaxation time is increased, i.e., $\tau_1\dot{\gamma}=0.25$, the parallel alignment of the lamellar plane starts to tilt away from the flow direction and tends to form the transverse alignment at intermediate shear strain. It tends to form the tilted parallel alignment when the shear strain is large, Fig. 3(b). When the deformation of the chain coils is even larger, i.e., $\tau_1\dot{\gamma}=0.75$, the transverse alignment is further observed, Fig. 3(c). However, this transverse alignment is also not very stable and is undulating in the $x-y$ plane. One important fact is that the appearance of the transverse alignment needs higher terminal Rouse relaxation time compared with that for shallow quench.

B. The evolution of correlation lengths

The details of the morphological evolution can be more quantitatively characterized by the correlation lengths of $R(x,t)$, $R(y,t)$, and $R(z,t)$ defined by Eq. (23), which are shown in Fig. 4. The evolution of these correlation lengths describes the domain growth and the detailed pathways of forming different morphologies.

For the cases of shallow quench ($\chi N=12.0$), when $\tau_1\dot{\gamma}=0$ and $\dot{\gamma}=0.001\,\mathrm{s}^{-1}$, the perpendicular alignment is observed as shown in Fig. 2(a). The evolution of the correlation length in this case is shown in Fig. 4(a). It is seen from Fig. 4(a) that $R(x,t)$ and $R(y,t)$ increase while $R(z,t)$ decreases with increase of shear strain. At large strain, $R(x,t)$ and $R(y,t)$ are much higher than $R(z,t)$. It should be mentioned that the value of $R(z,t)$ at large strain corresponds to the lamella thickness. All of these observations reveal that the perpendicular lamella alignment is achieved.

It can also be seen from Fig. 4(a) that, when the chain relaxation time ($\tau_1\dot{\gamma}=0.25$) is increased, the chain stretching effects just begin to come into play and $R(z,t)$ increases and oscillates while $R(x,t)$ keeps almost constant when shear strain is larger than 2. The evolution behavior of $R(y,t)$ oscillates around a constant. It is noted that, at large strain, $R(x,t)$ reaches the value of lamella thickness while $R(y,t)$ reaches the value of undulation period, which is larger than the lamella thickness. This result is consistent with the morphology shown in Fig. 2(b). When the chain relaxation time is even higher ($\tau_1\dot{\gamma}=0.75$), it could be imagined that the chain will be more severely stretched and the transverse lamella alignment will more easily appear. The evolution of the correlation lengths for this case supports this conjecture. It is seen that, in this case, $R(z,t)$ increases much faster than the case with shorter chain relaxation time. One very important feature of these two cases is that $R(z,t)$ and $R(y,t)$ oscillate with the shear strain. We must point out that this oscillation behavior is objective and cannot be eliminated by averaging over the independent simulations. Therefore, we would like to assign this oscillation to the undulation of the lamellae. The details of this process can be seen from Fig. 5. The shear flow field stretches the diblock copolymer chains along the flow direction. At the same time, the thermodynamic potential drives the system to phase separation. Combining these two effects, it is easy to understand the appearance of the transverse lamella alignment. However, the transversely stacked lamellae under steady shear flow are not stable and they will be deformed under the shear flow. Therefore, it is seen from Fig. 5 that, under steady shear flow, the transversely aligned lamellae are first undulated. Then, the part of the undulated lamellae with higher curvature, i.e., the higher surface tension, will connect to the similar part of their nearest-neighboring lamellae to form the restructured lamellae with smaller curvature, which costs less interfacial energy. This bending and connecting process is responsible for the oscillations observed in the evolution of the correlation lengths.

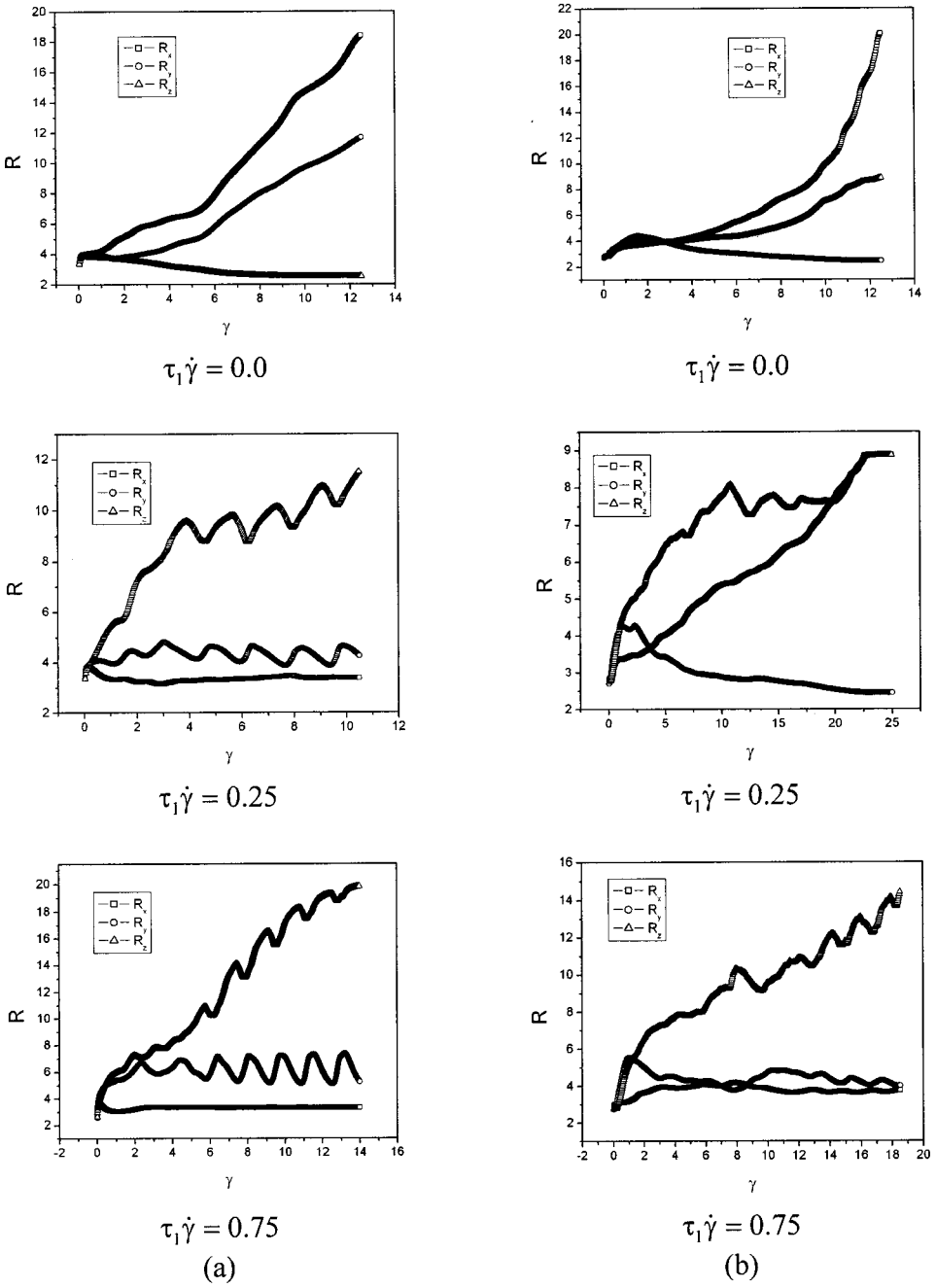

FIG. 4. Evolution of the average domain size (R_x, R_y, and R_z) of the morphology in the velocity, shear gradient, and vorticity directions for different $\tau_1\dot{\gamma}$ and quench depth χN (a) 12.0, (b) 20.0. The shear rate is $\dot{\gamma} = 0.001\,\mathrm{s}^{-1}$.

It is seen from Fig. 4(b) that, for the case of deep quench ($\chi N = 20.0$), when $\tau_1\dot{\gamma} = 0$ and $\dot{\gamma} = 0.001\,\mathrm{s}^{-1}$, the $R(x,t)$ and $R(z,t)$ increase while $R(y,t)$ decreases with the increase of shear strain. At large strain, $R(x,t)$ and $R(z,t)$ are much larger than $R(y,t)$, which corresponds to the lamella thickness at large strain. All of these observations reveal that the parallel lamella alignment is achieved. When the chain relaxation time is increased ($\tau_1\dot{\gamma} = 0.25$ and 0.75), the transverse alignment starts to appear and the evolution of the correlation lengths is quite similar to that shown in Fig. 4(a). However, the appearance of the transverse alignment requires higher chain relaxation time. Due to the same reason, the oscillation of the correlation lengths can be seen but the amplitude is not as high as that for shallow quench.

V. CONCLUSIONS

In this paper, the effects of steady shear flow-induced coil deformation on the morphology and dynamics of microphase separation in diblock copolymer systems are investigated based on Rouse model. Through the numerical simulation, the following conclusions can be drawn.

(1) The ODT temperature will increase with $\tau_1\dot{\gamma}$, and temperature-like parameter Δ change following the relations of $\Delta \sim (\tau_1\dot{\gamma})^{1.0}$ when $\tau_1\dot{\gamma} \leqslant 1.0$, and it levels off when $\tau_1\dot{\gamma} \gg 1.0$.

(2) Under the steady shear flow with $\dot{\gamma} = 0.001\,\mathrm{s}^{-1}$, the perpendicular alignment (with the lamella normal perpendicular to the flow direction, x, and parallel to the vorticity

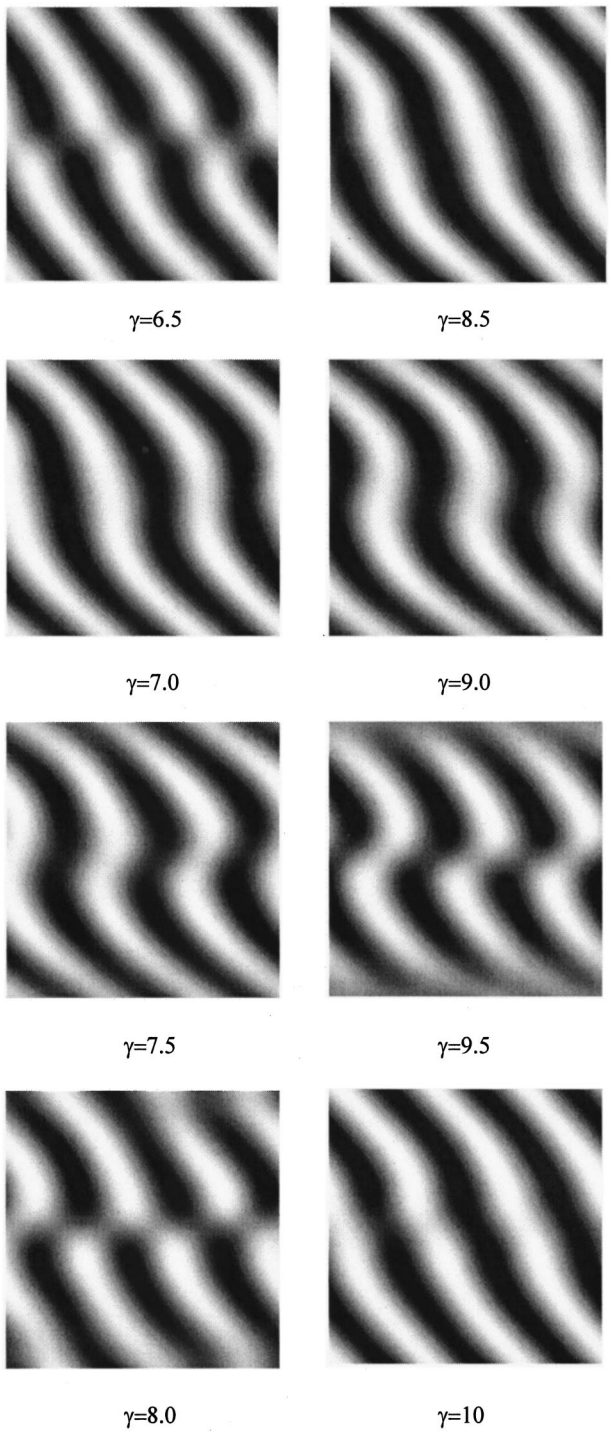

FIG. 5. The details of the undulation process in the $x-y$ plane for Fig. 2(b). The axes x and y are in the horizontal and vertical directions, respectively.

direction, z) is observed for short Rouse terminal relaxation time and shallow quench depth ($\chi N=12.0$). However, for $\chi N=12.0$, the transverse lamella alignment (with the lamella normal parallel to the flow direction, x) is observed for longer terminal relaxation time ($\tau_1\dot{\gamma}=0.75$) at the same shear rate ($\dot{\gamma}=0.001\,\mathrm{s}^{-1}$).

(3) It is found that the transverse alignment is not stable under steady shear flow and thus the lamella is undulating in the $x-y$ plane during flow. The detailed process of undulation is analyzed based on the snapshot of simulated morphologies and the evolution of the correlation lengths.

(4) For the case of deep quench ($\chi N=20.0$) and $\dot{\gamma}=0.001\,\mathrm{s}^{-1}$, the system with short Rouse terminal relaxation time prefers the parallel lamella alignment (the lamella normal is parallel to the velocity gradient direction, y). However, the transverse lamella alignment can be observed again when the Rouse terminal relaxation time is long enough. Moreover, for deep quench, the formation of the transverse alignment requires higher Rouse terminal relaxation time than that of shallow quench.

ACKNOWLEDGMENTS

This work is subsidized by the Special Funds for Major State Basic Research Projects (No. G1999064800), NSF of China. Partial financial support from The Shanghai Commission of S&T is also acknowledged.

[1] *Physics of Complex and Supermolecular Fluids*, edited by S. A. Safran and N. A. Clark (Wiley, New York, 1987).
[2] *Micelles, Membranes, Microemulsions, and Monolayers*, edited by W. M. Gelbart, A. Ben-Shaul, and D. Roux (Springer, Berlin, 1993).
[3] L. Leibler, Macromolecules **13**, 1602 (1980).
[4] G. H. Fredrickson and E. Helfand, J. Chem. Phys. **87**, 697 (1987).
[5] T. Ohta and K. Kawassaki, Macromolecules **19**, 2621 (1986).
[6] T. Ohta and K. Kawassaki, Macromolecules **23**, 2413 (1990).
[7] K. Almdal, J. H. Rosedale, F. S. Bates, G. D. Wignall, and G. H. Fredrickson, Phys. Rev. Lett. **65**, 112 (1990).
[8] W. W. Wayne, F. S. Bates, P. L. Lodge, K. Almdal, K. Mortensen, and G. H. Fredrickson, J. Chem. Phys. **108**, 2989 (1998).
[9] G. Hadziioannou and A. Skoulios, Macromolecules **15**, 258 (1982).
[10] K. I. Winey, S. S. Patel, R. G. Larson, and H. Watanabe, Macromolecules **26**, 2542 (1993).
[11] K. A. Koppi, M. Tirrell, F. S. Bates, K. Almdal, and R. H. Colby, J. Phys. II **2**, 1941 (1992).
[12] V. K. Gupta, R. Krishnamoorti, and J. A. Kornfield, Macromolecules **28**, 4313 (1995).
[13] Y. Zhang and U. Wiesner, J. Chem. Phys. **103**, 4784 (1995).
[14] G. H. Fredrickson, J. Chem. Phys. **85**, 5306 (1986).
[15] A. Onuki, K. Yamazaki, and K. Kawassaki, Ann. Phys. **131**, 217 (1981); A. Onuki and K. Kawassaki, Ann. Phys. **121**, 456 (1979); T. Imaeda, A. Onuki, and K. Yamazaki, Prog. Theor. Phys. **71**, 16 (1984).
[16] G. H. Fredrickson and R. G. Larson, J. Chem. Phys. **86**, 1553 (1987).
[17] A. Onuki, J. Chem. Phys. **87**, 3692 (1987).
[18] G. H. Fredrickson and E. Helfand, J. Chem. Phys. **89**, 5890 (1988).
[19] M. E. Cates and S. T. Milner, Phys. Rev. Lett. **62**, 1856 (1989).
[20] G. H. Fredrickson, J. Rheol. **38**, 1045 (1994).
[21] Y. Huang and M. Muthukumar, J. Chem. Phys. **107**, 5561 (1997).
[22] B. A. Wolf, Macromolecules **17**, 615 (1984).
[23] R. Horst and B. A. Wolf, Macromolecules **25**, 5291 (1992).
[24] R. Nafaile, A. B. Metzner, and K. F. Wissburn, Macromolecules **17**, 1187 (1984).
[25] S. M. Bhattacharjee, G. H. Fredrickson, and E. Helfand, J. Chem. Phys. **90**, 3305 (1989).
[26] N. Pistoor and K. Binder, Colloid Polym. Sci. **266**, 132 (1988).
[27] F. Qiu, J. Ding, and Y. Yang, Phys. Rev. E **58**, R1230 (1998).
[28] F. Qiu, H. Zhang, and Y. Yang, J. Chem. Phys. **108**, 9529 (1998).
[29] P. E. Rouse, J. Chem. Phys. **21**, 1273 (1953).
[30] P. G. De Gennes, *Scaling Concepts in Polymer Physics* (Cornell University Press, Ithaca, NY, 1979).
[31] P. G. De Gennes, J. Chem. Phys. **72**, 4756 (1980).
[32] M. Doi and S. F. Edwards, *The Theory of Polymer Dynamics* (Clarendon, Oxford, 1986).
[33] H. L. Frisch, N. Pistoor, A. Sariban, and K. Binder, J. Chem. Phys. **89**, 5194 (1988).
[34] L. Q. Chen and J. Shen, Comput. Phys. Commun. **108**, 147 (1998).

[35] J. Zhu, L. Q. Chen, J. Shen, and V. Tikare, Phys. Rev. E **60**, 3564 (1999).
[36] F. Corberi, G. Gonnella, and A. Lamura, Phys. Rev. Lett. **83**, 4057 (1999); **81**, 3852 (1998).
[37] N. P. Rapapa and A. Bray, Phys. Rev. Lett. **83**, 3856 (1999).
[38] H. Zhang and Y. Yang, Sci. China, Ser. B: Chem. **40**, 53 (1997).
[39] Y. Zhang, U. Wiesner, Y. Yang, T. Pakula, and H. W. Spiess, Macromolecules **29**, 5427 (1996).